PET Imaging of Adenosine A_1 Receptors with ^{11}C-MPDX as an Indicator of Severe Cerebral Ischemic Insult

Tadashi Nariai, MD, PhD[1]; Yuhei Shimada, PhD[2]; Kiichi Ishiwata, PhD[3]; Tsukasa Nagaoka, MD[1]; Junichi Shimada, PhD[4]; Toshihiko Kuroiwa, MD, PhD[5]; Ken-Ichiro Ono, PhD[2]; Kikuo Ohno, MD, PhD[1]; Kimiyoshi Hirakawa, MD, PhD[1]; and Michio Senda, MD, PhD[3]

[1]Department of Neurosurgery, Tokyo Medical and Dental University, Tokyo, Japan; [2]Department of Veterinary Clinical Pathobiology, University of Tokyo, Tokyo, Japan; [3]Positron Medical Center, Tokyo Metropolitan Institute of Gerontology, Tokyo, Japan; [4]Pharmaceutical Research Laboratories, Kyowa Hakko Kogyo Co., Ltd., Tokyo, Japan; and [5]Department of Neuropathology, Tokyo Medical and Dental University, Tokyo, Japan

We examined whether measurement of the adenosine A_1 receptor (A1-R) with PET can predict the severity of ischemic brain damage using an occlusion and reperfusion model of the cat middle cerebral artery (MCA) and [1-methyl-^{11}C]8-dicyclopropylmethyl-1-methyl-3-propylxanthine (MPDX), a positron-emitting radioligand developed at our institution. **Methods:** Eighteen adult cats underwent PET measurement of cerebral blood flow (CBF), A1-R, central benzodiazepine receptor (BDZ-R), and glucose metabolism with ^{15}O-labeled water, MPDX, ^{11}C-flumazenil (FMZ), and ^{18}F-FDG, respectively. The right MCAs of 13 cats were transiently occluded via a transorbital approach with microvascular clips. CBF was measured before occlusion of MCA, during occlusion, and immediately after reperfusion. After CBF measurement, A1-R, BDZ-R, and ^{18}F-FDG uptake were serially measured in the order listed. Two months later, the degree of ischemic damage was evaluated by T2-weighted MR images obtained with an animal MRI system and by analysis of histologic specimens. Five cats that received no operations were used as controls. **Results:** The cats that underwent occlusion were divided into 3 groups: cats that did not survive the first day because of severe neurologic and systemic conditions ($n = 4$), cats that survived and had infarcted lesions in both the cortex and the striatum ($n = 3$), and cats that survived and had infarcted lesions only in the striatum ($n = 6$). CBF during occlusion of the MCA was significantly lower in all 3 ischemic groups than in the control group, but there was no significant difference among the ischemic groups. Right-to-left ratios of CBF and ^{18}F-FDG uptake did not significantly differ among the groups. MPDX binding and FMZ binding were significantly lower in the groups with severe ischemic insult than in the groups with little to no insult. **Conclusion:** The degree of decreased MPDX binding to A1-Rs after reperfusion was a sensitive predictor of severe ischemic insult. MPDX PET has good potential to become a suitable in vivo imaging technique for evaluating the function of adenosine and A1-Rs in relation to cerebral ischemia.

Key Words: PET; cerebral ischemia; adenosine A_1 receptor; cat; middle cerebral artery occlusion; glucose metabolism

J Nucl Med 2003; 44:1839–1844

Adenosine is an endogenous modulator in the brain known to play an important role in ischemic cerebral damage and in protection of the brain against it (*1–4*). Our laboratory recently developed several radioligands for PET imaging of the adenosine receptor system in the living brain (*5–11*). Of these, [1-methyl-^{11}C]8-dicyclopropylmethyl-1-methyl-3-propylxanthine (MPDX) is thought to be a promising PET ligand with selective and high affinity for adenosine A_1 receptors (A1-Rs) in the central nervous system (*6,10,12*). We postulated that in vivo PET would be a sensitive method for measuring the role of substrate adenosine and A1-Rs during cerebral ischemic events. In this report, we evaluate the A1-R in an occlusion and reperfusion model of the cat middle cerebral artery (MCA) with MPDX and an animal PET scanner. Changes in cerebral blood flow (CBF), cerebral glucose metabolism (cerebral metabolic rate of glucose, or CMRGlc), and benzodiazepine receptor (BDZ-R) were also quantified and simultaneously analyzed to clarify the significance of A1-R quantification to cerebral ischemia.

MATERIALS AND METHODS

Experimental and Postoperative Procedures

Eighteen adult IOC cats weighing 3–4 kg were purchased from IFFA CREDO for use in the experiments. After injection of thiopental sodium (15 mg/kg intravenously) and atropine sulfate (0.05 mg/kg subcutaneously) to induce general anesthesia, the animals were intubated and the experimental procedure was started. The anesthesia was maintained with isoflurane (1.5%–2.0%), and ventilation was maintained at the same inspiratory

Received Dec. 6, 2002; revision accepted May 20, 2003.

For correspondence or reprints contact: Tadashi Nariai, MD, PhD, Department of Neurosurgery, Tokyo Medical and Dental University, 1-5-45 Yushima, Bunkyo-ku, Tokyo 113-8519, Japan.

E-mail: nariai.nsrg@tmd.ac.jp

volume (300 mL/min) with an animal respirator throughout the procedure. After the femoral artery and vein had been catheterized, the cat was positioned prone into a stereotactic head holder (Narishige) made of polymethyl methacrylate to minimize photon attenuation.

Electrocardiography findings, expiratory CO_2 concentration, and systemic arterial blood pressure measured with an arterial catheter were continuously monitored. Body temperature was recorded by a rectal thermometer and maintained at 38° by a heating pad and lamp with a thermocontroller.

The right MCAs of 13 cats were exposed via a transorbital approach and prepared for occlusion. The MCA was reopened after 60 min of occlusion. Animals were subjected to serial measurements of PET, as described below. Five cats that received no operation also underwent the PET measurement as controls.

After the experiment, one of us who was licensed as a veterinarian observed the neurologic and systemic physiologic parameters of the cats. Animals determined to have severe systemic and neurologic conditions due to the cerebral ischemia were euthanized by an intravenous overdose of pentobarbital immediately after completion of the PET scans without withdrawal of anesthesia. Animals determined to be in good condition were continuously monitored by a veterinarian with use of analgesics and antibiotics based on the postoperative management protocol of the veterinary hospital.

Two months after the initial experiment, the cats were evaluated by T2-weighted MRI using an animal MRI system (4.7-tesla Unity Plus SIS 200/330; Varian) while under the same anesthesia administered during the PET measurements. For examination of the structural changes corresponding to the PET and MRI findings, the animals were perfused transcardially with a buffered solution of 3% paraformaldehyde and 1% glutaraldehyde under pentobarbital anesthesia (50 mg/kg) shortly after the final MR image was obtained.

The brain was removed, cut sequentially into 3-mm-thick coronal sections, and placed in cooled fixative. The block corresponding to the MR images was chosen, immersed in buffered formalin, and processed for hematoxylin–eosin and Klüver–Barrera staining. A neuropathologist who had no knowledge of the results of the PET and MRI examinations analyzed each histologic specimen. Areas of infarction were traced on an image of each section scanned using a multipurpose scanner.

All experimental procedures were approved by the Animal Care and Use Committee of the Tokyo Metropolitan Institute of Gerontology (protocol 99064).

PET Scanning

PET measurement was performed with a model SHR-2000 PET camera designed for animal scanning (Hamamatsu Photonics Co.). When set in the *z*-motion mode, the camera provided 14 image slices with an interslice distance of 3.25 mm, an in-plane spatial resolution of 4.0 mm in full width at half maximum (FWHM), and an axial resolution of 5.0 mm in FWHM (*13*). The CBF of the cat was measured 3 times by intravenously injected $H_2{}^{15}O$: once 15 min before the MCA occlusion, once 5 min after the occlusion, and once 5 min after reperfusion. Next, the cat underwent a series of PET measurements of A1-R, BDZ-R, and CMRGlc using MPDX, ^{11}C-flumazenil (FMZ), and ^{18}F-FDG, respectively, all at the same slice positions. MPDX, FMZ, and ^{18}F-FDG were intravenously injected at 20, 195, and 315 min, respectively, after reperfusion. Transmission data were obtained with a rotating source to correct photon attenuation at 150–175 min after reperfusion. The tomographic images were reconstructed using a Butterworth filter with a cutoff frequency of 144 cycles per centimeter. The CBF was quantified by an intravenous injection of 200 MBq of $H_2{}^{15}O$ and a PET scan for 3 min starting at the time of injection. To obtain the intraarterial radioactivity of the tracer, β-probes were set into a specially prepared arteriovenous shunt. The details of this method have been published elsewhere (*14*). The static image of the A1-R distribution was acquired from 10 to 30 min after an injection of 200 MBq of MPDX (*10*). The static image of the BDZ-R was acquired from 10 to 30 min after an injection of 200 MBq of FMZ. Static imaging was deemed preferable to dynamic imaging in this experiment because the former minimized blood withdrawal. The 10- to 30-min time points selected for data collection were shown to optimally reflect the specific binding of both tracers in an analysis of data from the previous blocking experiment on healthy cats (*10,15*). The static image for the analysis of CMRGlc was acquired from 30 to 60 min after an injection of 100 MBq of ^{18}F-FDG.

PET Data Analysis

PET data analyses were performed on UNIX workstations (Silicon Graphics Inc.) using the Dr. View image analysis software system (Asahi Kasei Joho System). All PET images were coregistered with the MR image of each animal using the semiautomatic registration method described previously (*16*). For the control animals, the cortex in the MCA territory and striatum were defined on the MR image, the symmetric regions of interest (ROIs) were placed on the contralateral brain, and the PET parameters of these ROIs were computed on coregistered images. For the ischemic model, ROIs were placed by the method described below. A subtraction image expressing the reduction of CBF (the CBF during MCA occlusion minus that before occlusion) was constructed to determine the ischemic area, and the ROI was then manually placed on the cortical and striatal area. The control ROI was placed on the symmetric area over the contralateral (left) brain.

The right-to-left ratios (ischemic side to control side) of the CBF during and after the MCA occlusion, uptake of ^{18}F-FDG, and binding of MPDX and FMZ were compared among experimental groups using ANOVA and multiple comparisons with Bonferroni adjustment.

RESULTS

Animal Condition and Subgroup Definition

Four cats euthanized on the first day because of severe neurologic conditions (dilated pupils, loss of light reflex, and no recovery of spontaneous respiration) were classified as the group with the most severe ischemic insult (group D). Three of the 9 surviving cats exhibited infarctions on MRI and in the histologic examinations in both the cortex and the striatum (group Cor). The other 6 surviving cats exhibited infarcted lesions on MRI and in the histologic examination only in the striatum (group Str). The data on the ischemic animals were compared with those on the control cats (group N, $n = 5$).

Table 1 compares physiologic conditions among the 4 groups. Arterial blood pressure before the MCA occlusion showed no significant difference among the 4 groups, and

TABLE 1
Physiologic Parameters Among Subgroups

Parameter	Group N (n = 5)	Group D (n = 4)	Group Cor (n = 3)	Group Str (n = 6)
Mean ABP (mm Hg) at CBF measurement				
Initially	108.7 ± 5.1	88.5 ± 8.5	101.8 ± 21.4	91.8 ± 12.5
During MCA occlusion	—	84.3 ± 10.5	105.7 ± 18.8	95.5 ± 19.3
After reperfusion	—	93.8 ± 11.6	102.0 ± 20.0	89.0 ± 20.6
Mean end-expiratory CO_2 (%) throughout experiment	3.00 ± 0.84	3.78 ± 0.67	5.07 ± 0.32	3.62 ± 1.17
Mean body temperature (°C) throughout experiment	37.9 ± 0.25	38.0 ± 0.27	37.4 ± 0.45	37.7 ± 0.35
Blood glucose concentration (mg/dL) at ^{18}F-FDG scan	210.8 ± 47.8	244.0 ± 86.3	202.7 ± 39.9	204.2 ± 44.0

ABP = arterial blood pressure.
No significant difference in any parameters was found among subgroups (ANOVA, $P > 0.05$).

that during and after the MCA occlusion showed no significant differences among the 3 ischemic groups. Because the respiratory condition and body temperature were controlled, these parameters were well stabilized in single animals throughout the experimental procedure. Table 1 lists the average end-expiratory CO_2 concentration and average body temperature throughout all PET measurements. There were no significant differences in these parameters among the 4 groups. The blood glucose concentrations determined for the measurements of CMRGlc were also similar among the groups, although group D had a somewhat higher value.

Statistical Comparison of PET Parameters Among Groups

Figure 1 compares the PET parameters in the ischemic cerebral cortex among the groups. The CBF during occlusion of the MCA was significantly less in all 3 ischemic groups than in the control group. However, no statistically significant differences in the reduction rate were found among the 3 ischemic groups (Fig. 1A). The right-to-left ratios of CBF and ^{18}F-FDG uptake after reperfusion did not show any statistically significant differences among the 4 groups (Figs. 1B and 1C). Binding of MPDX to A1-R and binding of FMZ to BDZ-R were significantly less extensive in group D than in groups N and Str (Figs. 1D and 1E). Of the 2 receptor ligands examined, binding of MPDX in group D was reduced by a greater margin than was binding of FMZ in the same group (Figs. 1D and 1E).

Table 2 shows an analysis of the PET parameters in the striatum. As observed in the cortical data, there were no significant differences in CBF after reperfusion or in ^{18}F-FDG uptake among the groups. Furthermore, binding of MPDX to A1-Rs ($P < 0.01$) and binding of FMZ to BDZ-R ($P < 0.05$) were significantly less extensive in group D than in groups N and Str. Binding of MPDX in group D was reduced by a greater margin than was binding of FMZ.

Representative PET and MR Images

PET and MR images of representative animals in each group are shown in Figure 2. Larger reductions in binding of MPDX to A1-Rs and of FMZ to BDZ-Rs were always a sign that more severe ischemic damage would occur. How-

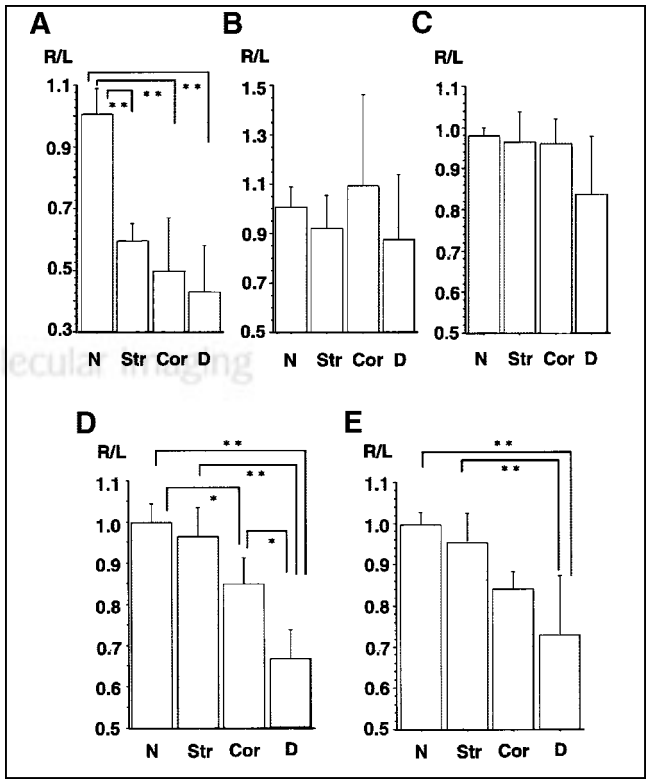

FIGURE 1. Bar graphs indicate PET parameters, including right-to-left ratio of CBF during occlusion of MCA (A), CBF after reperfusion (B), ^{18}F-FDG uptake as indicator of CMRGlc (C), MPDX binding to A1-Rs (D), and FMZ binding to BDZ-Rs (E), in ischemic cortex for each animal group. ANOVA and multiple comparisons between 6 pairs were performed by Bonferroni correction. CBF was reduced in all treated groups, but rate of reduction was not significantly different among them. No statistical difference among the 4 groups was found in right-to-left ratio of CBF or CMRGlc after reperfusion. MPDX binding was significantly lower in group D than in groups N, Str, and Cor. MPDX binding in group Cor was significantly lower than that in group N. FMZ binding was significantly lower in group D than in groups N and Str. Reductions of A1-Rs and BDZ-Rs were both good indicators of permanent ischemic insult, whereas reduction rate of MPDX binding to A1-Rs in group D was larger than that of FMZ binding to BDZ-Rs. *$P < 0.05$. **$P < 0.01$.

TABLE 2
PET Parameters in Ischemic Striatum (Ratio to Control Striatum)

Group	CBF (reperfusion) ($H_2{}^{15}O$)	CMRGlc (^{18}F-FDG)	A1-R (MPDX)	BDZ-R (FMZ)
N (n = 5)	0.93 ± 0.13	0.96 ± 0.09	0.99 ± 0.05	0.96 ± 0.09
Str (n = 6)	1.02 ± 0.20	0.92 ± 0.05	0.99 ± 0.06	0.93 ± 0.05
Cor (n = 3)	0.87 ± 0.20	0.82 ± 0.11	0.77 ± 0.22	0.78 ± 0.11
D (n = 4)	0.85 ± 0.21	0.72 ± 0.15	0.55 ± 0.22*	0.63 ± 0.25†

*$P < 0.01$ (significantly less than groups N and Str).
†$P < 0.05$ (significantly less than groups N and Str).

ever, in the case of CBF and CMRGlc, both reductions and increases can be signs of more severe damage, as exemplified by the second Cor animal. For this reason, it was difficult to foresee the fate of ischemic insult in individual animals on the basis of CBF and CMRGlc. Of the 2 receptor ligands, binding of MPDX to A1-Rs in the ischemic area was decreased by a larger margin than was binding of FMZ to BDZ-Rs, as seen in the animals in groups Cor and D. The widespread and prominent reduction in binding of MPDX to A1-Rs (too close to zero) was a sign that subsequent severe ischemic damage would occur, as seen in the nonsurviving animals of group D.

DISCUSSION

In this article, we have demonstrated that the rate of decrease in MPDX–A1-Rs binding measured with PET can be a good predictor of the degree of subsequent ischemic cerebral damage. Of the other parameters analyzed at the same time, the binding potential of FMZ to BZD-Rs was also good for early detection of ischemic lesions. CBF during arterial occlusion; CBF after reperfusion; and ^{18}F-FDG uptake, an indicator of CMRGlc, after reperfusion, were not good predictors of the degree of subsequent cerebral ischemic damage.

Both A1-R and BZD-R are well-recognized markers of the cellular component in the central nervous system. The

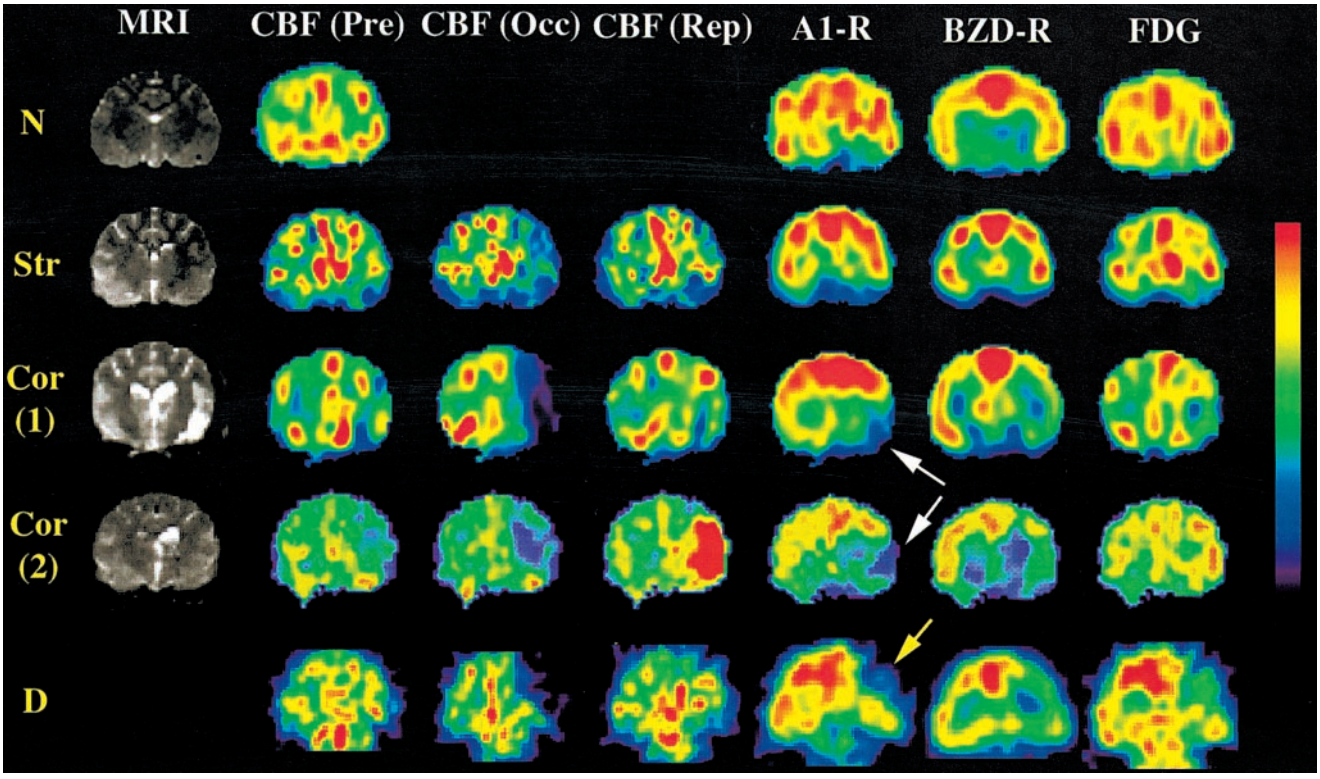

FIGURE 2. PET images display CBF before (Pre), during (Occ), and after (Rep) occlusion of MCA; uptake of ^{18}F-FDG; MPDX binding to A1-R; and FMZ binding to BZD-R for each animal group. Each PET image was coregistered with animal's own MR image, and corresponding coronal plane is shown for each parameter. (MRI was not performed for group D animals.) Group Str did not show any conspicuous abnormality in CMRGlc or radioligand binding to A1-R or BZD-R. Reduction in radioligand binding to A1-R and BZD-R was noted in both animals from group Cor. Of these 2 receptor ligands, area with decreased binding of MPDX to A1-R represented subsequent cortical infarction with better contrast (white arrows). However, CBF and CMRGlc both decreased in first Cor animal, whereas they both increased in second Cor animal. This may have explained poor performance of CBF and CMRGlc in predicting degree of ischemic insult soon after reperfusion. MPDX binding was reduced most prominently in group D, reaching almost zero (yellow arrow). FMZ binding and CMRGlc also decreased in group D, but not as prominently as MPDX binding. Color scale of images is displayed on right. Images CBF, A1-R, BZD-R, and ^{18}F-FDG are depicted in units of mL/min/100 mL, Bq/mL, Bq/mL, and standardized uptake value, respectively. Color scale for each animal was set so that control sides would indicate similar color level.

former is distributed in both the neurons and the glia (*17*), whereas the latter is distributed mainly in the neurons. Because of the abundant distribution of these 2 receptors in the neuronal body and synaptic terminal, they are often used as markers to represent neuronal integrity or synaptic projection (*18–20*). Accordingly, decreased binding of these receptors can be used as an indicator of significant damage in neuronal and glial function. On the other hand, the uncoupling of the CBF and CMRGlc (*21*), changes in the tracer distribution ratio (*22*), and the remote effects of functional deterioration (*23*) make the interpretation of CBF and CMRGlc in acute cerebral ischemia complex and the prediction of outcome using these parameters uncertain.

It has already been reported that the use of BZD-R as a marker of neuronal integrity is a superior method for early and accurate detection of cerebral damage in acute stages of ischemia (*24,25*). Our present results also confirmed that BZD-R imaging is superior to CBF and CMRGlc imaging. Further, the method of A1-R imaging used in the present study was also found to be superior in detecting ischemic damage, and the rate of reduction of A1-R binding in severe ischemia was larger than the rate of reduction of BZD-R binding in the cortex and the striatum. Although the limited number of animals used in the present study prevents us from drawing any conclusion on the superiority of one receptor ligand over another, we have provided evidence that A1-R imaging can evaluate the pathophysiology of cerebral ischemia from a different theoretic approach than that used in BZD-R imaging.

The ischemic condition has clearly been recognized to initiate a marked elevation of extracellular adenosine (*26–28*). In this condition, competition between intrinsic adenosine and an extrinsically injected tracer might cause decreased binding of MPDX to A1-Rs in the ischemic area, where the amount of adenosine released in the extracellular space far exceeds that released in the extracellular space of the nonischemic area. The degree of reduction in accumulation of extrinsic tracer may be a reliable indicator of an increased concentration of intrinsic substances, and this possibility has prompted PET studies to measure the release of intrinsic neurotransmitters by injecting positron-emitting receptor ligands (*29*). No report indicates that an endogenous substance is released and competes with FMZ during ischemia. Because BZD-R is considered to be a selective marker of neurons, the discrepancy between A1-R and BDZ-R imaging observed in the group with severe ischemic insult may have been partly attributable to the increased release of endogenous adenosine while the neuron was still preserved.

If this hypothesis stands, A1-R imaging by PET may provide a new method to monitor not only the extent of already damaged neuronal integrity but also the severity of the ongoing cerebral ischemic insult. At the stage when adenosine is accumulated in the extracellular space before the appearance of fatal cerebral edema, the interaction between neurotoxic and neuroprotective mechanisms is fully working through the adenosine and glutamate receptor systems (*3,30–33*). Therefore, there may still be a therapeutic window for manipulating such a neuroprotective mechanism through adenosine receptors (*1,2,34–36*). A1-R imaging during acute ischemia may be useful to determine whether such an intensive management procedure for neuronal protection is indicated.

In interpreting the data of the present study, one should bear in mind that the result may have been influenced by the order of the imaging protocol. A1-R imaging was performed immediately after reperfusion, and BDZ-R imaging was performed after complete decay of the MPDX radioactivity, that is, about 2 h after the A1-R imaging. The concentration of released endogenous substance rapidly changes during the reperfusion stage, and the increased endogenous substances might have influenced A1-R imaging much more than they did BDZ-R imaging. However, the accuracy of imaging performed 2 h earlier in predicting the final outcome well supports the usefulness of A1-R imaging in acute cerebral ischemia.

Now that we have completed PET A1-R imaging in the preclinical condition in the primate brain (*12*), application of this method in the human brain may soon be possible. Adenosine has been postulated to play neuroprotective roles not only in cerebral ischemia but also in neurotrauma and epilepsy (*37–39*). We therefore speculate that PET A1-R imaging might have good potential to become a powerful new technique for evaluating and treating various neurologic disorders.

CONCLUSION

We have examined whether a newly developed imaging method, PET of A1-Rs, can be applied to the evaluation of cerebral ischemia using an occlusion and reperfusion model of the cat MCA. The results indicated that the degree of decreased MPDX binding to A1-Rs after reperfusion was a sensitive predictor of severe ischemic insult. MPDX PET has good potential to become a suitable in vivo imaging technique for evaluating the function of adenosine and A1-Rs in relation to cerebral ischemia. This method may become a clinically useful diagnostic tool for early and precise detection of human cerebral ischemic disease.

ACKNOWLEDGMENTS

This work was supported by grants-in-aid 10671287 and 12671343 for scientific research from the Japanese Ministry of Education, Culture, Sports, Science, and Technology. We thank Keiichi Oda, Shin-ichi Ishii, and Miyoko Ando for technical support with the experimental procedure.

REFERENCES

1. Rudolphi KA, Schubert P, Parkinson FE, Fredholm BB. Neuroprotective role of adenosine in cerebral ischaemia. *Trends Pharmacol Sci.* 1992;13:439–445.
2. Sweeney MI. Neuroprotective effects of adenosine in cerebral ischemia: window of opportunity. *Neurosci Biobehav Rev.* 1997;21:207–217.

3. von Lubitz DK. Adenosine and cerebral ischemia: therapeutic future or death of a brave concept? *Eur J Pharmacol.* 1999;371:85–102.
4. Pearson T, Nuritova F, Caldwell D, Dale N, Frenguelli BG. A depletable pool of adenosine in area CA1 of the rat hippocampus. *J Neurosci.* 2001;21:2298–2307.
5. Furuta R, Ishiwata K, Kiyosawa M, et al. Carbon-11-labeled KF15372: a potential central nervous system adenosine A1 receptor ligand. *J Nucl Med.* 1996;37: 1203–1207.
6. Noguchi J, Ishiwata K, Furuta R, et al. Evaluation of carbon-11 labeled KF15372 and its ethyl and methyl derivatives as a potential CNS adenosine A1 receptor ligand. *Nucl Med Biol.* 1997;24:53–59.
7. Ishiwata K, Noguchi J, Wakabayashi S, et al. ^{11}C-Labeled KF18446: a potential central nervous system adenosine A2a receptor ligand. *J Nucl Med.* 2000;41: 345–354.
8. Noguchi J, Ishiwata K, Wakabayashi S, et al. Evaluation of carbon-11-labeled KF17837: a potential CNS adenosine A2a receptor ligand. *J Nucl Med.* 1998; 39:498–503.
9. Wakabayashi S, Nariai T, Ishiwata K, et al. A PET study of adenosine A1 receptor in anesthetized monkey brain. *Nucl Med Biol.* 2000;27:401–406.
10. Shimada Y, Ishiwata K, Kiyosawa M, et al. Mapping adenosine A(1) receptors in the cat brain by positron emission tomography with [^{11}C]MPDX. *Nucl Med Biol.* 2002;29:29–37.
11. Ishiwata K, Takai H, Nonaka H, Ishii S, Simada J, Senda M. Synthesis and preliminary evaluation of a carbon-11-labeled adenosine transporter blocker [^{11}C]KF21562. *Nucl Med Biol.* 2001;28:281–285.
12. Ishiwata K, Nariai T, Kimura Y, et al. Preclinical studies on [^{11}C]MPDX for mapping adenosine A1 receptors by positron emission tomography. *Ann Nucl Med.* 2002;16:377–382.
13. Watanabe M, Uchida H, Okada H, et al. A high resolution PET for animal studies. *IEEE Trans Med Imaging.* 1992;1992:577–580.
14. Sakiyama Y, Sato A, Senda M, Ishiwata K, Toyama H, Schmidt RF. Positron emission tomography reveals changes in global and regional cerebral blood flow during noxious stimulation of normal and inflamed elbow joints in anesthetized cats. *Exp Brain Res.* 1998;118:439–446.
15. Shimada Y, Kiyosawa M, Nariai T, et al. Quantitative in vivo measurement of central benzodiazepine receptors in the brain of cats by use of positron-emission tomography and [^{11}C]flumazenil. *Am J Vet Res.* 2003;64:999–1002.
16. Shimada Y, Uemura K, Ardekani BA, et al. Application of PET-MRI registration techniques to cat brain imaging. *J Neurosci Methods.* 2000;101:1–7.
17. Hosli E, Hosli L. Receptors for neurotransmitters on astrocytes in the mammalian central nervous system. *Prog Neurobiol.* 1993;40:477–506.
18. Goodman RR, Kuhar MJ, Hester L, Snyder SH. Adenosine receptors: autoradiographic evidence for their location on axon terminals of excitatory neurons. *Science.* 1983;220:967–969.
19. Matus A, Pehling G, Wilkinson D. Gamma-aminobutyric acid receptors in brain postsynaptic densities. *J Neurobiol.* 1981;12:67–73.
20. Madar I, Scheffel U, Frost JJ. Transient increase in the in vivo binding of the benzodiazepine antagonist [^{3}H]flumazenil in deafferented visual areas of the adult mouse brain. *Synapse.* 1994;18:79–85.
21. Lassen NA. The luxury-perfusion syndrome and its possible relation to acute metabolic acidosis localised within the brain. *Lancet.* 1966;2:1113–1115.
22. Greenberg JH, Hamar J, Welsh FA, Harris V, Reivich M. Effect of ischemia and reperfusion on lambda of the lumped constant of the [^{14}C]deoxyglucose technique. *J Cereb Blood Flow Metab.* 1992;12:70–77.
23. Lenzi GL, Frackowiak RS, Jones T. Cerebral oxygen metabolism and blood flow in human cerebral ischemic infarction. *J Cereb Blood Flow Metab.* 1982;2:321–335.
24. Heiss WD, Graf R, Fujita T, et al. Early detection of irreversibly damaged ischemic tissue by flumazenil positron emission tomography in cats. *Stroke.* 1997;28:2045–2051.
25. Heiss WD, Kracht L, Grond M, et al. Early [^{11}C]flumazenil/H_2O positron emission tomography predicts irreversible ischemic cortical damage in stroke patients receiving acute thrombolytic therapy. *Stroke.* 2000;31:366–369.
26. Hagberg H, Andersson P, Lacarewicz J, Jacobson I, Butcher S, Sandberg M. Extracellular adenosine, inosine, hypoxanthine, and xanthine in relation to tissue nucleotides and purines in rat striatum during transient ischemia. *J Neurochem.* 1987;49:227–231.
27. Melani A, Pantoni L, Corsi C, et al. Striatal outflow of adenosine, excitatory amino acids, gamma-aminobutyric acid, and taurine in awake freely moving rats after middle cerebral artery occlusion: correlations with neurological deficit and histopathological damage. *Stroke.* 1999;30:2448–2454.
28. Matsumoto K, Graf R, Rosner G, Shimada N, Heiss WD. Flow thresholds for extracellular purine catabolite elevation in cat focal ischemia. *Brain Res.* 1992; 579:309–314.
29. Koepp MJ, Gunn RN, Lawrence AD, et al. Evidence for striatal dopamine release during a video game. *Nature.* 1998;393:266–268.
30. Erdemli G, Xu YZ, Krnjevic K. Potassium conductance causing hyperpolarization of CA1 hippocampal neurons during hypoxia. *J Neurophysiol.* 1998;80: 2378–2390.
31. Fowler JC. Adenosine antagonists delay hypoxia-induced depression of neuronal activity in hippocampal brain slice. *Brain Res.* 1989;490:378–384.
32. Katchman AN, Hershkowitz N. Adenosine antagonists prevent hypoxia-induced depression of excitatory but not inhibitory synaptic currents. *Neurosci Lett.* 1993;159:123–126.
33. Pearson T, Frenguelli BG. Volume-regulated anion channels do not contribute extracellular adenosine during the hypoxic depression of excitatory synaptic transmission in area CA1 of rat hippocampus. *Eur J Neurosci.* 2000;12:3064–3066.
34. Phillis JW, O'Regan MH. Deoxycoformycin antagonizes ischemia-induced neuronal degeneration. *Brain Res Bull.* 1989;22:537–540.
35. Gidday JM, Fitzgibbons JC, Shah AR, Kraujalis MJ, Park TS. Reduction in cerebral ischemic injury in the newborn rat by potentiation of endogenous adenosine. *Pediatr Res.* 1995;38:306–311.
36. de Mendonca A, Sebastiao AM, Ribeiro JA. Adenosine: does it have a neuroprotective role after all? *Brain Res Brain Res Rev.* 2000;33:258–274.
37. Nilsson P, Hillered L, Ponten U, Ungerstedt U. Changes in cortical extracellular levels of energy-related metabolites and amino acids following concussive brain injury in rats. *J Cereb Blood Flow Metab.* 1990;10:631–637.
38. Headrick JP, Bendall MR, Faden AI, Vink R. Dissociation of adenosine levels from bioenergetic state in experimental brain trauma: potential role in secondary injury. *J Cereb Blood Flow Metab.* 1994;14:853–861.
39. Dunwiddie TV. Adenosine and suppression of seizures. *Adv Neurol.* 1999;79: 1001–1010.